frontiers in Physics

ORIGINAL RESEARCH
published: 03 June 2020
doi: 10.3389/fphy.2020.00201

Check for updates

RETRACTED: Numerical Treatment for 3D Squeezed Flow in a Rotating Channel With Soret and Dufour Effects

Abdullah K. Alzahrani[1], *Malik Zaka Ullah*[1] *and Taseer Muhammad*[2]*

[1] Department of Mathematics, Faculty of Science, King Abdulaziz University, Jeddah, Saudi Arabia, [2] Department of Mathematics, College of Sciences, King Khalid University, Abha, Saudi Arabia

This article examines magnetohydrodynamic three-dimensional (3D) squeezed flow by a rotating permeable channel subject to Dufour and Soret impacts. Impact of viscous dissipation is also considered. An applied magnetic field is considered subject to electrically conducting viscous fluid. The change from the non-linear partial differential framework to the non-linear ordinary differential framework is assumed into position by utilizing appropriate variables. Governing differential frameworks are computed numerically by shooting method. Numerical results have been achieved by considering numerous values of emerging flow parameters. Contributions of influential parameters on physical quantities are studied thoroughly. Surface drag coefficients and mass and heat transport rates are also processed and examined. Furthermore, the concentration and temperature distributions are reduced for larger values of Soret number. The prime interest of presented study is to model and examine the Dufour and Soret aspects in concentration and energy expressions. To our knowledge, no such analysis has been addressed in the literature yet.

Keywords: squeezing flow, viscous dissipation, MHD, Dufour and Soret effects, rotating channel

RETRACTED

OPEN ACCESS

Edited by:
Marin I. Marin,
Transilvania University of Braşov, Romania

Reviewed by:
Khadija Maqbool,
International Islamic University, Islamabad, Pakistan
Sorin Vlase,
Transilvania University of Braşov, Romania
M. M. Bhatti,
Shandong University of Science and Technology, China
Nicolae I. Pop,
Solid Mechanics Institute of the Romanian Academy, Romania

***Correspondence:**
Taseer Muhammad
taseer_qau@yahoo.com;
tasgher@kku.edu.sa

Specialty section:
This article was submitted to Mathematical Physics, a section of the journal Frontiers in Physics

Received: *23 November 2019*
Accepted: *05 May 2020*
Published: *03 June 2020*

Citation:
Alzahrani AK, Ullah MZ and Muhammad T (2020) Numerical Treatment for 3D Squeezed Flow in a Rotating Channel With Soret and Dufour Effects. Front. Phys. 8:201. doi: 10.3389/fphy.2020.00201

1. INTRODUCTION

Flow squeezed by two parallel surfaces is an attractive region of research embraced by recent researchers. The presence of squeezed flow in the designing applications having liquid metal grease, polymer, and sustenance ventures is in charge of this premium. Squeezing flow can be utilized in displaying the grease framework. Stefan [1] has started the exploration on lubrication approximation. Squeezed flow of power-law liquid between parallel disks is examined by Leider and Bird [2]. Hamza and MacDonald [3] discussed the effect of suction/blowing in the squeezed flow. MHD unsteady squeezed flow between two parallel surfaces is discussed by Bhattacharyya and Pal [4]. Fully developed free-convection micropolar fluid flow in a vertical channel is provided by Chamkha et al. [5]. Rashidi et al. [6] introduced the investigation of axisymmetric and two-dimensional squeezed flows between parallel walls. Homotopic perturbation solution for MHD squeezed flow between parallel disks is addressed by Domairry and Aziz [7]. Hayat et al. [8] explored squeezed flow of second-grade liquid between parallel disks. Three-dimensional squeezed flow in a rotating channel with lower stretchable permeable plate is examined by Munawar et al. [9]. Freidoonimehr et al. [10] investigated solution in a rotating channel by taking three-dimensional squeezed nanofluid flow. Few relevant examinations on squeezed flows can be seen through attempts [11–15].

Simultaneous presence of mass and heat transfer in a moving liquid gives more intricate nature that the fluxes and driving potentials convey between them. It has been seen that temperature gradients and also concentration gradients can produce energy flux. The diffusion-thermo (Dufour) impact is characterized as the heat transport because of concentration gradient while the thermal-diffusion (Soret) impact is the mass transport because of temperature gradient. Mass and heat transport related examinations uncovered the smaller order of magnitude of the Dufour and Soret impacts when contrasted with the impacts of Fourier's and Fick's law and are neglected much of the time. These impacts are critical in nuclear waste disposal, hydrology, geothermal energy, petrology, etc. Soret impact is utilized for partition of isotope and in mixture between gases with almost small and medium sub-atomic weights (H_2, He) and (N_2, air) separately. Dufour impact can't be ignored in view of its considerable magnitude [16]. Rashidi et al. [17] explained convective MHD flow by a rotating disk subject to diffusion-thermo and thermal-diffusion impacts. Dufour and Soret features in magnetohydrodynamic Casson liquid flow over an extending surface is proposed by Hayat et al. [18]. Turkyilmazoglu and Pop [19] examined the Soret impact in natural convection unsteady flow subject to thermal radiation and heat generation. Properties of Dufour and Soret in buoyancy-driven MHD flow by a stretching surface is addressed by Pal and Mondal [20]. Hayat et al. [21] explored Dufour and Soret impacts in mixed convection peristaltic transport containing nanoliquid by considering slip and Joule heating. Some relevant examinations on Dufour and Soret effects can be seen through attempts [22–25].

Keeping the above discussion in mind, the present article is organized for magnetohydrodynamic three-dimensional (3D) squeezed flow of viscous liquid in a rotating permeable channel subject to Dufour and Soret effects. Viscous dissipation is also considered. Non-linear partial differential systems are simplified via appropriate transformations to the non-linear ordinary differential systems. Shooting technique is used in order to construct the numerical solution of non-linear flow problem. Salient features of fluid flow and mass and heat transfer are further examined.

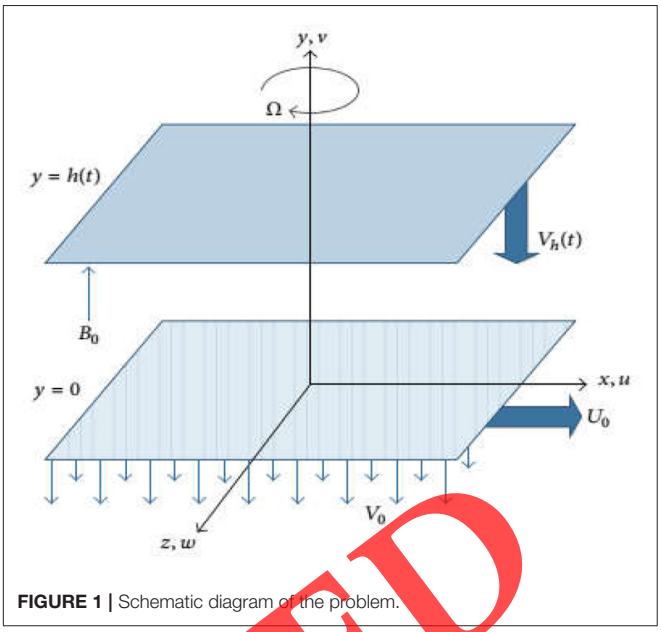

FIGURE 1 | Schematic diagram of the problem.

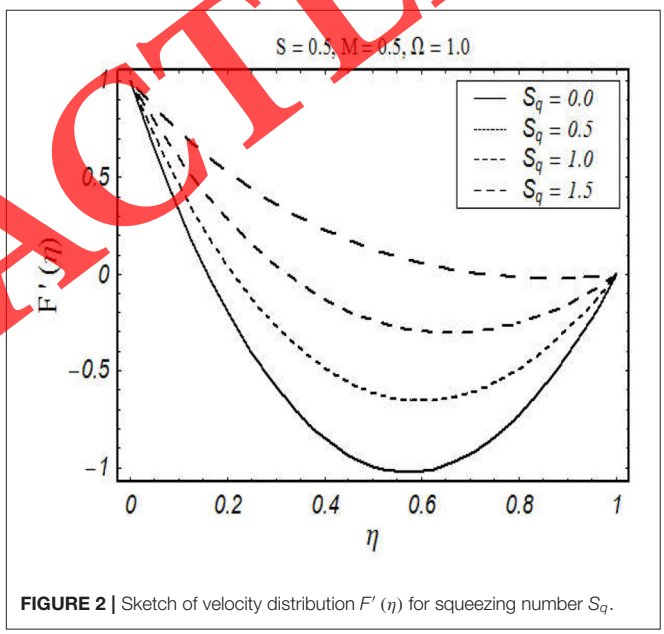

FIGURE 2 | Sketch of velocity distribution $F'(\eta)$ for squeezing number S_q.

RETRACTED

2. PROBLEM FORMULATION

We examine unsteady three dimensional squeezing flow of viscous liquid between two parallel plates which are separated by a distance $\sqrt{\nu(1-\gamma t)/a}$. Upper plate at $y = h(t) = \sqrt{\nu(1-\gamma t)/a}$ is moving with velocity $-\frac{\gamma}{2}\sqrt{\frac{\nu}{a(1-\gamma t)}}$ and the lower permeable plate at $y = 0$ is stretched with velocity $(ax/1-\gamma t)$ in which t is always less than $1/\gamma$ (see **Figure 1**). An angular velocity $\Omega = \omega j/1-\gamma t$ has been utilized by the fluid and the channel to rotate about $y-$axis while the lower plate sucks the flow with velocity $-V_0/1-\gamma t$. Magnetic field of strength $(B_0/1-\gamma t)$ is employed in $y-$direction [26–32]. The thermophysical characteristics of under discussion fluid are taken to be constant. The governing equations in rotating frame of reference are defined by

$$\nabla.\mathbf{V} = 0, \tag{1}$$

$$\rho\left[\frac{\partial \mathbf{V}}{\partial t} + (\mathbf{V}.\nabla)\,\mathbf{V} + 2\Omega \times \mathbf{V}\right] = \nabla.\tau + \mathbf{J} \times \mathbf{B}, \tag{2}$$

in which τ stands for Cauchy stress tensor, $\mathbf{V}$ for velocity field, $\mathbf{J}$ for magnetic flux and $\mathbf{B}$ for current density.

In component form, the resulting expressions of mass, momentum, energy, and concentration in the absence of thermal

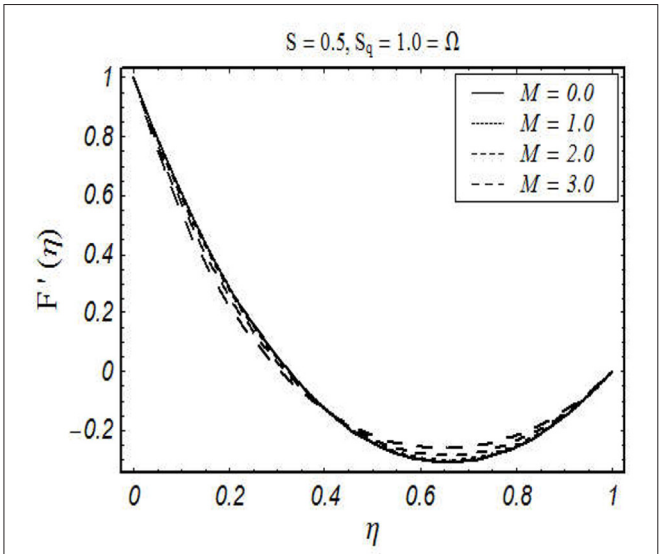

FIGURE 3 | Sketch of velocity distribution $F'(\eta)$ for magnetic number M.

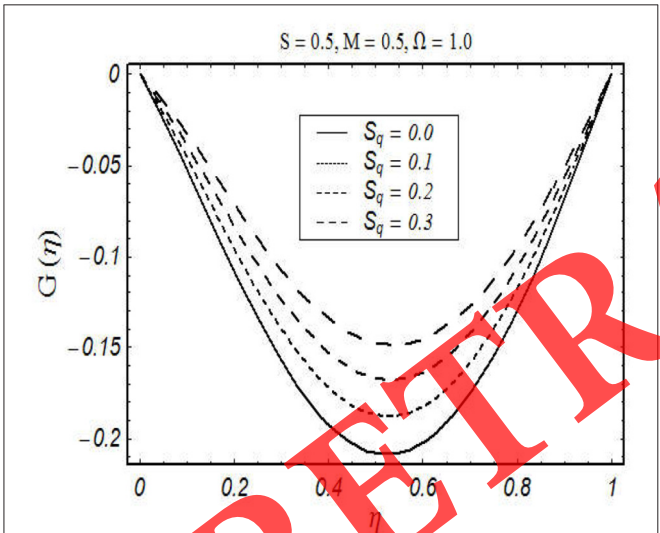

FIGURE 4 | Sketch of velocity distribution $G(\eta)$ for squeezing number S_q.

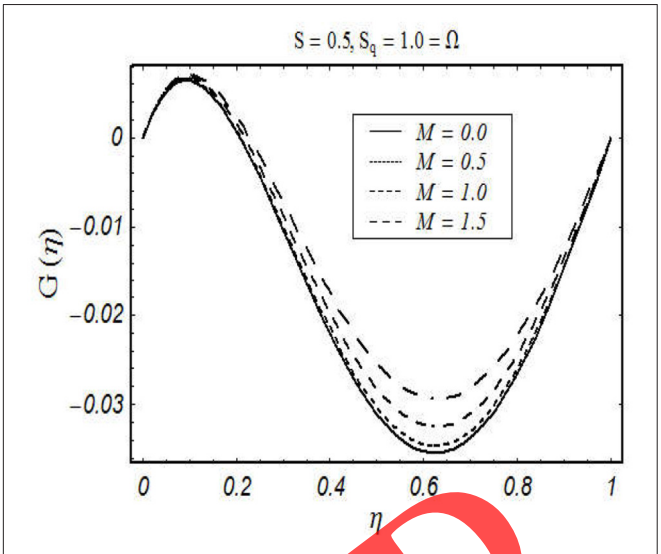

FIGURE 5 | Sketch of velocity distribution $G(\eta)$ for magnetic number M.

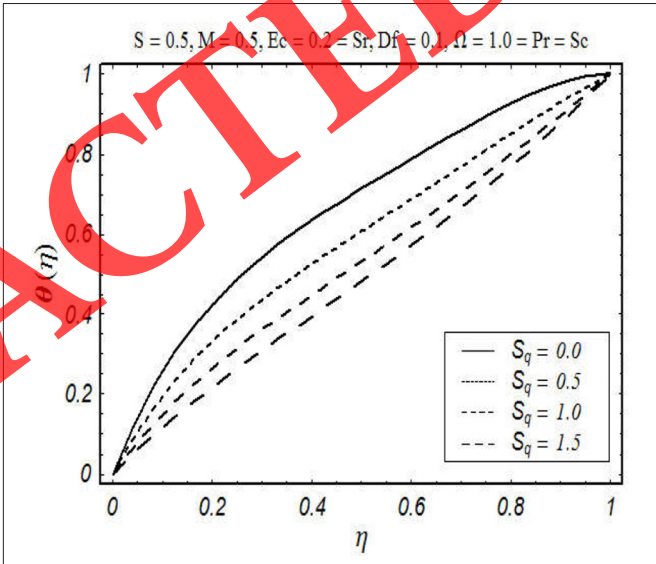

FIGURE 6 | Sketch of temperature distribution $\theta(\eta)$ for squeezing number S_q.

RETRACTED

radiation are [9, 25]:

$$\frac{\partial u}{\partial x}+\frac{\partial v}{\partial y}=0, \tag{3}$$

$$\frac{\partial u}{\partial t}+u\frac{\partial u}{\partial x}+v\frac{\partial u}{\partial y}+2\frac{\omega}{1-\gamma t}w=-\frac{1}{\rho}\frac{\partial p}{\partial x}+\nu\left(\frac{\partial^2 u}{\partial x^2}+\frac{\partial^2 u}{\partial y^2}\right)-\frac{\sigma B_0^2}{\rho\,(1-\gamma t)}u, \tag{4}$$

$$\frac{\partial v}{\partial t}+u\frac{\partial v}{\partial x}+v\frac{\partial v}{\partial y}=-\frac{1}{\rho}\frac{\partial p}{\partial y}+\nu\left(\frac{\partial^2 v}{\partial x^2}+\frac{\partial^2 v}{\partial y^2}\right), \tag{5}$$

$$\frac{\partial w}{\partial t}+u\frac{\partial w}{\partial x}+v\frac{\partial w}{\partial y}-2\frac{\omega}{1-\gamma t}u=\nu\left(\frac{\partial^2 w}{\partial x^2}+\frac{\partial^2 w}{\partial y^2}\right)-\frac{\sigma B_0^2}{\rho\,(1-\gamma t)}w, \tag{6}$$

$$\frac{\partial T}{\partial t}+u\frac{\partial T}{\partial x}+v\frac{\partial T}{\partial y}=\alpha_m^*\left(\frac{\partial^2 T}{\partial x^2}+\frac{\partial^2 T}{\partial y^2}\right)+\frac{Dk_T}{c_s c_p}\left(\frac{\partial^2 C}{\partial x^2}+\frac{\partial^2 C}{\partial y^2}\right)+\frac{\nu}{c_p}\left[4\left(\frac{\partial u}{\partial x}\right)^2+\left(\frac{\partial w}{\partial x}\right)^2+\left(\frac{\partial w}{\partial y}\right)^2+\left(\frac{\partial u}{\partial y}+\frac{\partial v}{\partial x}\right)^2\right], \tag{7}$$

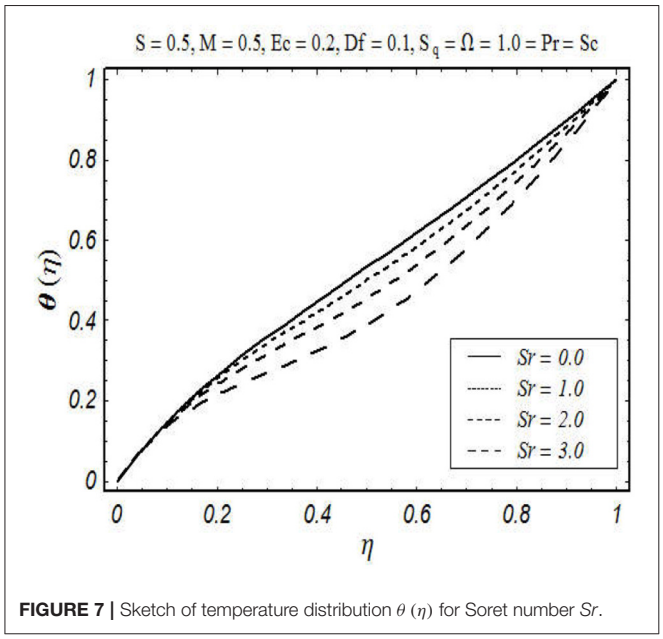

FIGURE 7 | Sketch of temperature distribution $\theta(\eta)$ for Soret number *Sr*.

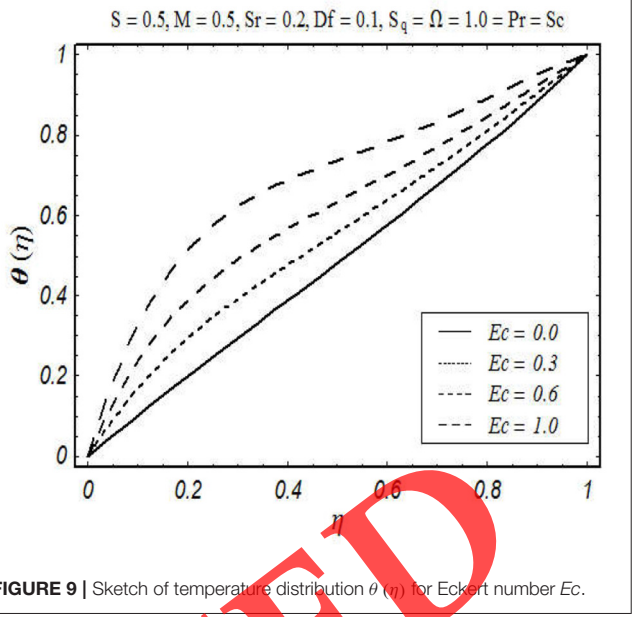

FIGURE 9 | Sketch of temperature distribution $\theta(\eta)$ for Eckert number *Ec*.

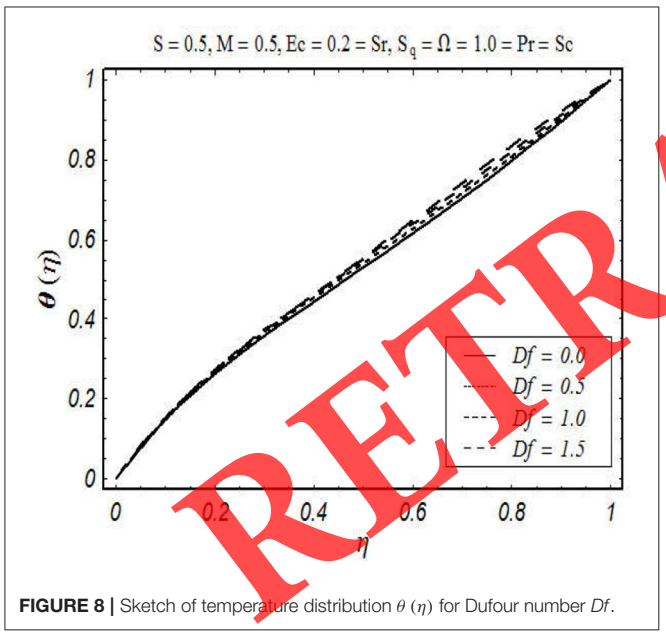

FIGURE 8 | Sketch of temperature distribution $\theta(\eta)$ for Dufour number *Df*.

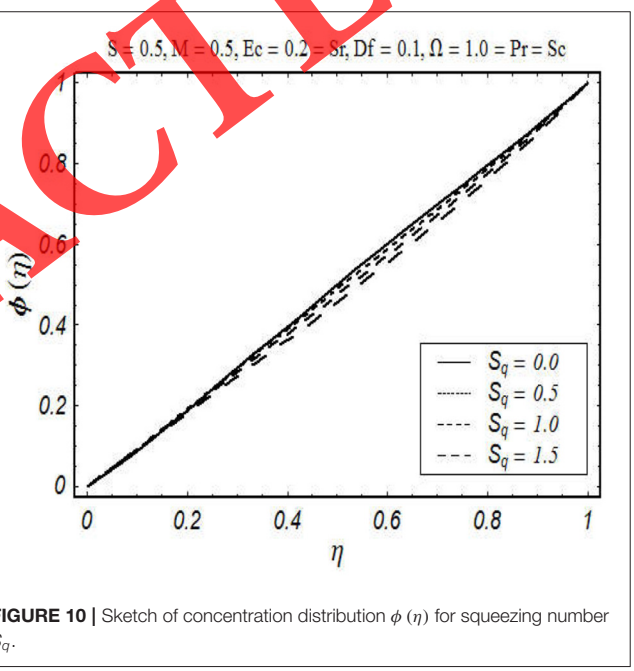

FIGURE 10 | Sketch of concentration distribution $\phi(\eta)$ for squeezing number S_q.

RETRACTED

$$\frac{\partial C}{\partial t}+u\frac{\partial C}{\partial x}+v\frac{\partial C}{\partial y}=D\left(\frac{\partial^2 C}{\partial x^2}+\frac{\partial^2 C}{\partial y^2}\right)+\frac{Dk_T}{T_m}\left(\frac{\partial^2 T}{\partial x^2}+\frac{\partial^2 T}{\partial y^2}\right). \tag{8}$$

Here u, v and w represent velocities in $x-$, $y-$ and $z-$directions respectively whereas μ, ρ, $\nu\,(=\mu/\rho)$, p and σ stand for dynamic viscosity, density, kinematic viscosity, pressure and electrical conductivity respectively, D for mass diffusion coefficient, α_m^* for thermal diffusivity, T for temperature, k_T for thermal-diffusion, c_s for concentration susceptibility, c_p for specific heat, C for concentration and T_m for fluid mean temperature. Subjected boundary conditions are [9, 12]:

$$\left.\begin{array}{c} u=U_0=\frac{ax}{1-\gamma t},\ v=-\frac{V_0}{1-\gamma t},\ w=0,\\ T=T_0,\ C=C_0 \text{ at } y=0,\\ u=0,\ v=V_h=\frac{dh}{dt}=-\frac{\gamma}{2}\sqrt{\frac{\nu}{a(1-\gamma t)}},\ w=0,\\ T=T_0+\frac{T_0}{1-\gamma t},\ C=C_0+\frac{C_0}{1-\gamma t} \text{ at } y=h(t), \end{array}\right\} \tag{9}$$

in which stretching rate of the lower plate, suction, injection, temperature and concentration at the lower plate are symbolized

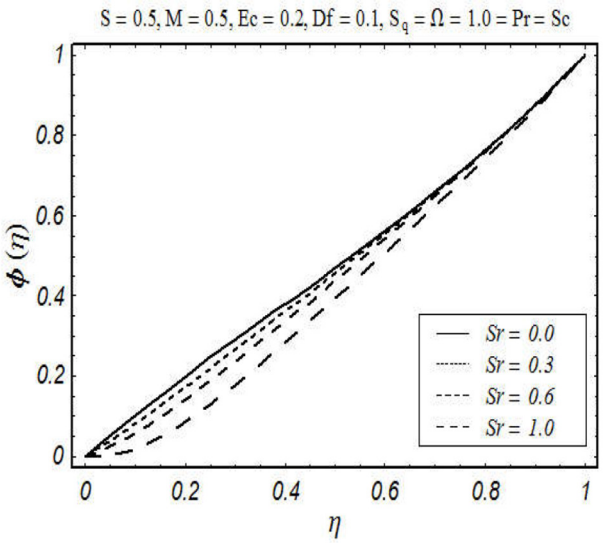

FIGURE 11 | Sketch of concentration distribution $\phi(\eta)$ for Soret number *Sr*.

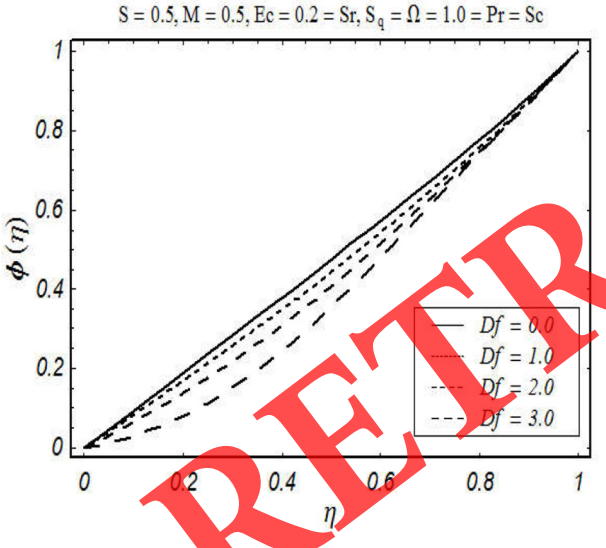

FIGURE 12 | Sketch of concentration distribution $\phi(\eta)$ for Dufour number *Df*.

by a, $V_0 > 0$, $V_0 < 0$, T_0 and C_0 respectively. Selecting [9, 12]:

$$\left.\begin{aligned} u = U_0 F'(\eta),\ v = -\sqrt{\tfrac{av}{1-\gamma t}}F(\eta),\ w = U_0 G(\eta), \\ T = T_0 + \tfrac{T_0}{1-\gamma t}\theta(\eta),\ C = C_0 + \tfrac{C_0}{1-\gamma t}\phi(\eta),\ \eta = \tfrac{y}{h(t)}. \end{aligned}\right\} \quad (10)$$

Pressure gradient is eliminated from Equations (4) and (5) and Equation (3) is now verified while Equations (4) − (9) have been reduced to

$$F^{iv} + FF''' - F'F'' - \frac{S_q}{2}\left(3F'' + \eta F'''\right) - 2\Omega G' - M^2 F'' = 0, \quad (11)$$

TABLE 1 | Numerical data for friction drag coefficients for varying S, Ω, S_q and M.

S	Ω	S_q	M	$F''(1)$	$G'(1)$
0.0	1.0	1.0	0.5	−1.19012	−0.27982
0.5				1.80841	0.14897
1.0				4.59809	0.62470
0.5	0.0	1.0	0.5	1.80818	0.00000
	1.0			1.80841	0.14897
	2.0			1.80917	0.29668
0.5	1.0	0.0	0.5	4.74572	0.70238
		0.5		3.29900	0.40198
		1.0		1.80841	0.14897
0.5	1.0	1.0	0.0	1.81491	0.15205
			0.5	1.80841	0.14897
			1.0	1.78950	0.14043

TABLE 2 | Numerical data for local Nusselt number and local Sherwood number for varying S, Ω, S_q, M, Ec, Sr, Df, Sc, and Pr.

S	Ω	S_q	M	Ec	Sr	Df	Pr	Sc	$\theta'(1)$	$\phi'(1)$
0.0	1.0	1.0	0.5	0.2	0.2	0.1	1.0	1.0	1.15515	1.24613
0.5									1.03914	1.20302
1.0									0.38216	1.26397
0.5	0.0	1.0	0.5	0.2	0.2	0.1	1.0	1.0	1.03962	1.20289
	1.0								1.03914	1.20302
	2.0								1.03771	1.20342
0.5	1.0	0.0	0.5	0.2	0.2	0.1	1.0	1.0	0.02447	1.08841
		0.5							0.62744	1.12944
		1.0							1.03914	1.20302
0.5	1.0	1.0	0.0	0.2	0.2	0.1	1.0	1.0	1.03779	1.20315
			0.5						1.03914	1.20302
			1.0						1.04303	1.20265
0.5	1.0	1.0	0.5	0.0	0.2	0.1	1.0	1.0	1.19673	1.17548
				0.5					0.80275	1.24434
				1.0					0.40878	1.31320
0.5	1.0	1.0	0.5	0.2	0.0	0.1	1.0	1.0	1.03780	1.21384
					0.5				1.04129	1.18554
					1.0				1.04531	1.15261
0.5	1.0	1.0	0.5	0.2	0.2	0.0	1.0	1.0	1.03914	1.20302
						0.3			0.99784	1.21096
						0.5			0.95318	1.21955
0.5	1.0	1.0	0.5	0.2	0.2	0.1	0.5	1.0	1.01525	1.20921
							1.0		1.03914	1.20302
							1.5		1.07059	1.19549
0.5	1.0	1.0	0.5	0.2	0.2	0.1	1.0	0.5	1.04879	1.10260
								1.0	1.03914	1.20302
								1.5	1.02969	1.30137

RETRACTED

$$G'' + FG' - F'G - \frac{S_q}{2}\left(2G + \eta G'\right) + 2\Omega F' - M^2 G = 0, \quad (12)$$

$$\theta'' + \Pr\left(F\theta' - \frac{S_q}{2}\left(2\theta + \eta\theta'\right) + Ec\left(F''^2 + G'^2\right) + Df\phi''\right) = 0, \quad (13)$$

TABLE 3 | Comparative values of $F''(1)$ and $G'(1)$ for value of Ω when $S = M = 0.5$ and $S_q = 0$.

	Present results		Munawar et al. [9]	
Ω	$F''(1)$	$G'(1)$	$F''(1)$	$G'(1)$
2.0	4.82359	1.40319	4.8235909	1.4031897

$$\phi'' + Sc\left(F\phi' - \frac{S_q}{2}\left(2\phi + \eta\phi'\right) + Sr\theta''\right) = 0, \tag{14}$$

$$F = S,\ F' = 1,\ G = 0,\ \theta = 0,\ \phi = 0 \text{ at } \eta = 0, \tag{15}$$

$$F = \frac{S_q}{2},\ F' = 0,\ G = 0,\ \theta = 1,\ \phi = 1 \text{ at } \eta = 1. \tag{16}$$

Here Ec stands for Eckert number, Ω for rotation parameter, S for suction/blowing parameter, M for magnetic number, Pr for Prandtl number, S_q for squeezing number, Sr for Soret number, Sc for Schmidt number and Df for Dufour number. These parameters are stated by

$$\left.\begin{aligned} S_q = \frac{\gamma}{a},\ \Omega = \frac{\omega}{a},\ M^2 = \frac{\sigma B_0^2}{\rho a},\ S = \frac{V_0}{ah(t)},\ \Pr = \frac{\nu}{\alpha_m^*}, \\ Ec = \frac{U_0^2(1-\gamma t)}{c_p T_0},\ Df = \frac{Dk_T C_0}{c_s c_p \nu T_0},\ Sc = \frac{\nu}{D},\ Sr = \frac{Dk_T T_0}{T_m \nu C_0}. \end{aligned}\right\} \tag{17}$$

Expressions of friction drag coefficients are given by

$$C_{fx} = \frac{\tau_{wx}|_{y=h(t)}}{\rho V_h^2} = \frac{\mu\left(\frac{\partial u}{\partial y} + \frac{\partial v}{\partial x}\right)_{y=h(t)}}{\rho V_h^2}, \tag{18}$$

and

$$C_{fz} = \frac{\tau_{wz}|_{y=h(t)}}{\rho V_h^2} = \frac{\mu\left(\frac{\partial w}{\partial y}\right)_{y=h(t)}}{\rho V_h^2}. \tag{19}$$

Friction drag coefficients in non-dimensional scale are

$$\frac{\gamma^2}{4a^2} C_{fx} = (Re_x)^{1/2} F''(1), \tag{20}$$

and

$$\frac{\gamma^2}{4a^2} C_{fz} = (Re_x)^{1/2} G'(1). \tag{21}$$

The non-dimensional forms of local Nusselt and Sherwood numbers are stated below:

$$Nu_x = -\frac{x}{(T_w - T_0)} \left.\frac{\partial T}{\partial y}\right|_{y=h(t)} = -(Re_x)^{1/2} \theta'(1), \tag{22}$$

$$Sh_x = -\frac{x}{(C_w - C_0)} \left.\frac{\partial C}{\partial y}\right|_{y=h(t)} = -(Re_x)^{1/2} \phi'(1), \tag{23}$$

in which local Reynolds number is signified by $Re_x = U_0 x/\nu$.

3. SOLUTION METHODOLOGY

By utilizing acceptable boundary conditions on system of the equations, a numerical solution is established employing NDSolve in Mathematica. Shooting method is employed via NDSolve. This method is very friendly in case of small step-size featuring negligible error. As a consequence, both the y and x varied uniformly by a step-size of 0.01 [26, 33–35].

4. NUMERICAL RESULTS AND DISCUSSION

This section elaborates impacts of different flow variables like magnetic number M, Eckert number Ec, squeezing number S_q, Soret number Sr and Dufour number Df on velocities $F'(\eta)$ and $G(\eta)$, temperature $\theta(\eta)$ and concentration $\phi(\eta)$. **Figure 2** depicts that how squeezing number S_q affects velocity distribution $F'(\eta)$. It is seen that the velocity distribution $F'(\eta)$ is depreciated near the permeable plate where suction impacts are superior. Pressure which increases the flow has been developed due to the mobility of the upper plate toward a stretching permeable plate. Mass conservation constrain has been mollified by incrementing velocity distribution $F'(\eta)$ near the upper plate. **Figure 3** demonstrates that how the velocity distribution is get effected by magnetic parameter M. Here the velocity distribution is decayed by enhancing M for $(0 \leq \eta \leq 0.4)$ while opposite trend is seen when $(0.4 \leq \eta \leq 1)$. Physically by increasing magnetic parameter M, the velocity and its gradient are decreased. Therefore the mass conservation constraint is satisfied by introducing the same mass flow rate. In MHD flow, we consider that a cross flow behavior is generated by increasing fluid velocity in the central region which results in balancing of fluid velocity decrement in the wall regions. **Figure 4** depicts variation in velocity distribution $G(\eta)$ for varying squeezing number S_q. It is noted that by enhancing S_q, an enhancement is appeared in velocity distribution $G(\eta)$ and this increment is more prominent at central zone of channel. **Figure 5** is displayed to depict the influence of magnetic number M on velocity distribution $G(\eta)$. Greater values of magnetic parameter M constitutes a lower velocity distribution $G(\eta)$. **Figure 6** depicts the impact of squeezing number S_q on temperature distribution $\theta(\eta)$. An increment in squeezing number S_q leads to weaker temperature $\theta(\eta)$. **Figures 7, 8** are sketched to examine that how temperature distribution is get effected by Soret Sr and Dufour Df numbers. From these figures, temperature distribution is weaker for larger Sr while higher trend is seen for larger Df. **Figure 9** displays that higher Eckert parameter Ec leads to stronger temperature distribution $\theta(\eta)$. From **Figure 10**, we clearly examined that a lower concentration distribution $\phi(\eta)$ is produced by considering higher squeezing parameter S_q. **Figures 11, 12** represent that change in concentration $\phi(\eta)$ for varying Soret and Dufour numbers respectively. Here we seen that an increase in Sr and Df show decreasing behavior for concentration distribution $\phi(\eta)$. **Table 1** is tabulated in order to analyze the numerical computations of friction drag coefficients $F''(1)$ and $G'(1)$ for varying Ω, S, M, and S_q. Here

RETRACTED

we examined that friction drags are reduced for the greater values of M and S_q while it enhances by incrementing S. **Table 2** presents numerical estimations of mass and heat transport rates for varying S, Ec, Ω, M, S_q, Sr, Pr, Df, and Sc. Here we concluded that mass and heat transport rates are higher when larger estimations of S_q are considered. **Table 3** is developed to validate present data with previous published data in a limiting case. Here we seen that present numerical solution has good agreement with previous solution by Munawar et al. [9] in a limiting sense.

5. CONCLUSIONS

Magnetohydrodynamic three-dimensional (3D) squeezed flow of viscous liquid in a rotating permeable channel subject to Dufour and Soret effects is discussed. Shooting method is used in order to construct the numerical solution of resulting non-linear flow problem. Larger squeezing number S_q demonstrates increasing behavior for both velocity components $F'(\eta)$ and $G(\eta)$. Magnetic parameter M has quite similar effects for both velocity components $F'(\eta)$ and $G(\eta)$. By increasing the Eckert parameter Ec, an enhancement is observed in temperature distribution $\theta(\eta)$. Opposite trend is seen in temperature distribution $\theta(\eta)$ for larger estimations of Dufour and Soret numbers. Concentration distribution $\phi(\eta)$ is decreasing functions of Dufour and Soret numbers. The Dufour impact is characterized as the heat transport because of concentration gradient while the Soret impact is the mass transport because of temperature gradient. Heat and mass transport related examinations uncovered the smaller order of magnitude of the Dufour and Soret impacts when contrasted with the impacts of Fourier's and Fick's law and are neglected much of the time. These impacts are critical in nuclear waste disposal, hydrology, geothermal energy, petrology, etc. The present work provides an inspiration for future developments on topic in the regimes of melting heat transfer, variable sheet thickness, Cattaneo–Christov heat flux and Joule heating.

DATA AVAILABILITY STATEMENT

The datasets generated for this study are available on request to the corresponding author.

AUTHOR CONTRIBUTIONS

All authors listed have made a substantial, direct and intellectual contribution to the work, and approved it for publication.

ACKNOWLEDGMENTS

This project was funded by the Deanship of Scientific Research (DSR) at King Abdulaziz University, Jeddah, Saudi Arabia under grant no. G:456-130-1440. The authors, therefore, acknowledge with thanks DSR for technical and financial support.

RETRACTED

REFERENCES

1. Stefan MJ. Versuch Uber die scheinbare adhesion, Akademie der Wissenschaften in Wien. *Mathematik-Naturwissen.* (1874) **69**:713.
2. Leider PJ, Bird RB. Squeezing flow between parallel disks, I. Theoretical analysis. *Ind Eng Chem Fundam.* (1974) **13**:336–41. doi: 10.1021/i160052a007
3. Hamza EA, MacDonald DA. A fluid film squeezed between two plane surfaces. *J Fluid Mech.* (1981) **109**:147–60. doi: 10.1017/S0022112081000980
4. Bhattacharyya S, Pal A. Unsteady MHD squeezing flow between two parallel plates. *Ing Arch.* (1990) **60**:274–81. doi: 10.1007/BF00577864
5. Chamkha AJ, Grosan T, Pop I. Fully developed free convection of a micropolar fluid in a vertical channel. *Int Commun Heat Mass Transfer.* (2002) **29**:1119–27. doi: 10.1016/S0735-1933(02)00440-2
6. Rashidi MM, Shahmohamadi H, Dinarvand S. Analytic approximate solutions for unsteady two-dimensional and axisymmetric squeezing flows between parallel plates. *Math Prob Eng.* (2008) **2008**:935095. doi: 10.1155/2008/935095
7. Domairry G, Aziz A. Approximate analysis of MHD squeeze flow between two parallel disks with suction or injection by homotopy perturbation method. *Math Prob Eng.* (2009) **2009**:603916. doi: 10.1155/2009/603916
8. Hayat T, Yousaf A, Mustafa M, Obaidat S. MHD squeezing flow of second-grade fluid between two parallel disks. *Int J Numer Meth Fluids.* (2012) **69**:399–410. doi: 10.1002/fld.2565
9. Munawar S, Mehmood A, Ali A. Three-dimensional squeezing flow in a rotating channel of lower stretching porous wall. *Comput Math Appl.* (2012) **64**:1575–86. doi: 10.1016/j.camwa.2012.01.003
10. Freidoonimehr N, Rostami B, Rashidi MM, Momoniat E. Analytical modelling of three-dimensional squeezing nanofluid flow in a rotating channel on a lower stretching porous wall. *Math Prob Eng.* (2014) **2014**:692728. doi: 10.1155/2014/692728
11. Mahanthesh B, Gireesha BJ, Gorla RSR. Mixed convection squeezing three-dimensional flow in a rotating channel filled with nanofluid. *Int J Numer Methods Heat Fluid Flow.* (2016) **26**:1460–85. doi: 10.1108/HFF-03-2015-0087
12. Hayat T, Sajjad R, Alsaedi A, Muhammad T, Ellahi R. On squeezed flow of couple stress nanofluid between two parallel plates. *Results Phys.* (2017) **7**:553–61. doi: 10.1016/j.rinp.2016.12.038
13. Sin CS, Zheng L, Sin JS, Liu F, Liu L. Unsteady flow of viscoelastic fluid with the fractional K-BKZ model between two parallel plates. *Appl Math Modell.* (2017) **47**:114–27. doi: 10.1016/j.apm.2017.03.029
14. Muhammad T, Hayat T, Alsaedi A, Qayyum A. Hydromagnetic unsteady squeezing flow of Jeffrey fluid between two parallel plates. *Chin J Phys.* (2017) **55**:1511–22. doi: 10.1016/j.cjph.2017.05.008
15. Hayat T, Haider F, Muhammad T, Alsaedi A, Darcy-Forchheimer squeezed flow of carbon nanotubes with thermal radiation. *J Phys Chem Solids.* (2018) **120**:79–86. doi: 10.1016/j.jpcs.2018.04.016
16. Eckert ERG, Drake RM. *Analysis of Heat and Mass Transfer.* New York, NY: McGraw-Hill (1972).
17. Rashidi MM, Hayat T, Erfani E, Pour SAM, Hendi AA. Simultaneous effects of partial slip and thermal-diffusion and diffusion-thermo on steady MHD convective flow due to a rotating disk. *Commun Nonlinear Sci Numer Simulat.* (2011) **16**:4303–17. doi: 10.1016/j.cnsns.2011.03.015
18. Hayat T, Shehzad SA, Alsaedi A. Soret and Dufour effects on magnetohydrodynamic (MHD) flow of Casson fluid. *Appl Math Mech Eng Ed.* (2012) **33**:1301–12. doi: 10.1007/s10483-012-1623-6
19. Turkyilmazoglu M, Pop I. Soret and heat source effects on the unsteady radiative MHD free convection flow from an impulsively started infinite vertical plate. *Int J Heat Mass Transfer.* (2012) **55**:7635–44. doi: 10.1016/j.ijheatmasstransfer.2012.07.079
20. Pal D, Mondal H. Influence of Soret and Dufour on MHD buoyancy-driven heat and mass transfer over a stretching sheet in porous media with temperature-dependent viscosity. *Nuclear Eng Design.* (2013) **256**:350–7. doi: 10.1016/j.nucengdes.2012.08.015
21. Hayat T, Abbasi FM, Al-Yami M, Monaquel S. Slip and Joule heating effects in mixed convection peristaltic transport of nanofluid with Soret and Dufour effects. *J Mol Liq.* (2014) **194**:93–9. doi: 10.1016/j.molliq.2014.01.021

22. Hayat T, Muhammad T, Shehzad SA, Alsaedi A. Soret and Dufour effects in three-dimensional flow over an exponentially stretching surface with porous medium, chemical reaction and heat source/sink. *Int J Numer Methods Heat Fluid Flow*. (2015) **25**:762–81. doi: 10.1108/HFF-05-2014-0137
23. Majeed A, Zeeshan A, Ellahi R. Chemical reaction and heat transfer on boundary layer Maxwell Ferro-fluid flow under magnetic dipole with Soret and suction effects. *Eng Sci Tech Int J*. (2017) **20**:1122–8. doi: 10.1016/j.jestch.2016.11.007
24. Hayat T, Ullah I, Muhammad T, Alsaedi A. Radiative three-dimensional flow with Soret and Dufour effects. *Int J Mech Sci*. (2017) **133**:829–37. doi: 10.1016/j.ijmecsci.2017.09.015
25. Farooq A, Ali R, Benim AC. Soret and Dufour effects on three dimensional Oldroyd-B fluid. *Phys A*. (2018) **503**:345–54. doi: 10.1016/j.physa.2018.02.204
26. Asma M, Othman WAM, Muhammad T, Mallawi F, Wong BR. Numerical study for magnetohydrodynamic flow of nanofluid due to a rotating disk with binary chemical reaction and Arrhenius activation energy. *Symmetry*. (2019) **11**:1282. doi: 10.3390/sym11101282
27. Ellahi R, Sait SM, Shehzad N, Mobin N. Numerical simulation and mathematical modeling of electro-osmotic Couette-Poiseuille flow of MHD power-law nanofluid with entropy generation. *Symmetry*. (2019) **11**:1038. doi: 10.3390/sym11081038
28. Alamri SZ, Khan AA, Azeez M, Ellahi R. Effects of mass transfer on MHD second grade fluid toward stretching cylinder: a novel perspective of Cattaneo-Christov heat flux model. *Phys Lett A*. (2019) **383**:276–81. doi: 10.1016/j.physleta.2018.10.035
29. Zeeshan A, Hussain F, Ellahi R, Vafai K. A study of gravitational and magnetic effects on coupled stress bi-phase liquid suspended with crystal and Hafnium particles down in steep channel. *J Mol Liq*. (2019) **286**:110898. doi: 10.1016/j.molliq.2019.110898
30. Alqahtani AM, Khan I. Time dependent MHD flow of non-Newtonian generalized Burgers' fluid (GBF) over a suddenly moved plate with generalized Darcy's law. *Front Phys*. (2020) **7**:214. doi: 10.3389/fphy.2019.00214
31. Sarafraz MM, Pourmehran O, Yang B, Arjomandi M, Ellahi R. Pool boiling heat transfer characteristics of iron oxide nano-suspension under constant magnetic field. *Int J Thermal Sci*. (2020) **147**:106131. doi: 10.1016/j.ijthermalsci.2019.106131
32. Bhatti MM, Shahid A, Abbas T, Alamri SZ, Ellahi R. Study of activation energy on the movement of gyrotactic microorganism in a magnetized nanofluids past a porous plate. *Processes*. (2020) **8**:328. doi: 10.3390/pr8030328
33. Marin M, Vlase S, Paun M. Considerations on double porosity structure for micropolar bodies. *AIP Adv*. (2015) **5**:037113. doi: 10.1063/1.4914912
34. Marin M, Nicaise S. Existence and stability results for thermoelastic dipolar bodies with double porosity. *Contin Mech Thermodyn*. (2016) **28**:1645–57. doi: 10.1007/s00161-016-0503-4
35. Marin M, Ellahi R, Chirilă A. On solutions of Saint-Venant's problem for elastic dipolar bodies with voids. *Carpathian J Math*. (2017) **33**:219–32. Available online at: https://www.jstor.org/stable/90017791

Conflict of Interest: The authors declare that the research was conducted in the absence of any commercial or financial relationships that could be construed as a potential conflict of interest.

Copyright © 2020 Alzahrani, Ullah and Muhammad. This is an open-access article distributed under the terms of the Creative Commons Attribution License (CC BY). The use, distribution or reproduction in other forums is permitted, provided the original author(s) and the copyright owner(s) are credited and that the original publication in this journal is cited, in accordance with accepted academic practice. No use, distribution or reproduction is permitted which does not comply with these terms.

RETRACTED

NOMENCLATURE

u, v, w	Velocity components	x, y, z	Coordinate axes
Ω	Angular velocity	B_0	Magnetic field strength
μ	Dynamic viscosity	ρ	Fluid density
ν	Kinematic viscosity	p	Pressure
σ	Electrical conductivity	V_0	Suction/blowing velocity
T	Temperature	C	Concentration
α_m^*	Thermal diffusivity	D	Mass diffusion coefficient
c_s	Concentration susceptibility	c_p	Specific heat
k_T	Thermal-diffusion	T_m	Fluid mean temperature
a	Stretching rate	t	Time
T_0	Temperature at lower plate	C_0	Concentration at lower plate
F', G	Dimensionless velocities	η	Dimensionless variable
θ	Dimensionless temperature	ϕ	Dimensionless concentration
S_q	Squeezing number	Ec	Eckert number
S	Suction/blowing parameter	M	Magnetic number
Ω	Rotation parameter	Pr	Prandtl number
Sc	Schmidt number	Sr	Soret number
Df	Dufour number	Nu_x	Local Nusselt number
τ_{wx}, τ_{wz}	Wall shear stresses	Sh_x	Local Sherwood number
C_{fx}, C_{fz}	Skin friction coefficients	Re_x	Local Reynolds number

RETRACTED